Carcinogenesis, 2020, Vol. 41, No. 12, 1648–1659

doi:10.1093/carcin/bgaa047
Advance Access publication July 25, 2020
Original Article

ORIGINAL ARTICLE

A polycyclic aromatic hydrocarbon-enriched environmental chemical mixture enhances AhR, antiapoptotic signaling and a proliferative phenotype in breast cancer cells

Larisa M.Gearhart-Serna[1,2,3], John B.Davis[4], Mohit Kumar Jolly[5,8], Nishad Jayasundara[3,6], Scott J.Sauer[1], Richard T.Di Giulio[3] and Gayathri R.Devi[1,2,7,*]

[1]Department of Surgery, Division of Surgical Sciences, [2]Department of Pathology, [3]Nicholas School of the Environment and [4]Department of Biology, Trinity School of Arts and Sciences, Duke University, Durham, NC 27710, USA, [5]Center for Theoretical Biological Physics, Rice University, Houston, TX 77005, USA, [6]School of Marine Sciences, University of Maine, Orono, ME 04469, USA and [7]Women's Cancer Program, Duke Cancer Institute, Duke University, Durham, NC 27710, USA
[8]Present address: Centre for BioSystems Science and Engineering, Indian Institute of Science, Bangalore, India

*To whom correspondence should be addressed. 2606 DUMC, Department of Surgery, Duke University School of Medicine, Durham, NC 27710, USA. Tel: (919) 668-0410; Email: gayathri.devi@duke.edu

Abstract

Emerging evidence suggests the role of environmental chemicals, in particular endocrine-disrupting chemicals (EDCs), in progression of breast cancer and treatment resistance, which can impact survival outcomes. However, most research tends to focus on tumor etiology and the effect of single chemicals, offering little insight into the effects of realistic complex mixture exposures on tumor progression. Herein, we investigated the effect of a polycyclic aromatic hydrocarbon (PAH)-enriched EDC mixture in a panel of normal and breast cancer cells and in a tumor organoid model. Cells or organoids in culture were treated with EDC mixture at doses estimated from US adult intake of the top four PAH compounds within the mixture from the National Health and Nutrition Examination Survey database. We demonstrate that low-dose PAH mixture (6, 30 and 300 nM) increased aryl hydrocarbon receptor (AhR) expression and CYP activity in estrogen receptor (ER) positive but not normal mammary or ER-negative breast cancer cells, and that upregulated AhR signaling corresponded with increased cell proliferation and expression of antiapoptotic and antioxidant proteins XIAP and SOD1. We employed a mathematical model to validate PAH-mediated increases in AhR and XIAP expression in the MCF-7 ER-positive cell line. Furthermore, the PAH mixture caused significant growth increases in ER-negative breast cancer cell derived 3D tumor organoids, providing further evidence for the role of a natural-derived PAH mixture in enhancing a tumor proliferative phenotype. Together, our integrated cell signaling, computational and phenotype analysis reveals the underlying mechanisms of EDC mixtures in breast cancer progression and survival.

Introduction

Breast cancer is the most common cancer among women worldwide, and in the USA one in eight women will develop invasive breast cancer (1). Although multimodal therapies continue to increase patient survival, aggressive locally advanced breast cancers are characterized by high rates of residual disease, treatment resistance and recurrence, leading to the worst survival outcomes among breast cancers and therefore present a major clinical challenge (2). Breast cancer outcomes are influenced by patient and tumor characteristics as well as access to quality treatment (3–5); however, emerging epidemiological

Received: October 7, 2019; **Revised:** April 21, 2020; **Accepted:** July 24, 2020

Abbreviations

AhR	aryl hydrocarbon receptor
BaP	benzo[*a*]pyrene
EDC	endocrine-disrupting chemical
ER	estrogen receptor
PAH	polycyclic aromatic hydrocarbon

cancer studies suggest a role of environmental chemical exposures, in particular endocrine-disrupting chemicals (EDCs), in breast cancer development and biology (6–11). EDCs are present in a wide variety of human products and emissions (12–14). Chemical screening by the U.S. Environmental Protection Agency shows that nearly 87 000 EDCs have some effect on mammary growth, development and maintenance (15), which has led to the U.S. Federal Interagency Breast Cancer and Environmental Research Coordinating Committee emphasizing the need to investigate mechanisms of EDC influence on breast cancer (16).

Polycyclic aromatic hydrocarbons (PAHs) are prototypical EDCs present ubiquitously in the environment as they are released via incomplete organic fuel combustion from anthropogenic and natural sources including tobacco smoke, charred or smoked meat, industrial byproduct emissions, forest fires, volcanic eruptions and even contaminated food (17). Both ambient air and human serum PAH levels have previously been linked to increased breast cancer risk (18,19). Some PAHs target the aryl hydrocarbon receptor (AhR) pathway (20) and subsequently upregulate cytochrome p450 enzymes (CYPs) which facilitate their metabolism, although CYP activity can be cell line specific in terms of CYP1A1 or CYP1B1 dominating PAH metabolism (21–23). Importantly, PAH compounds such as benzo[*a*]pyrene (BaP) are also known to generate DNA-reactive metabolites and upregulate reactive oxygen species. This subsequently upregulates superoxide dismutase (SOD) antioxidant enzymes, including in breast cells (24). We have previously observed that increased expression of antioxidants like SOD1 (25,26) causes clonal expansion of aggressive, drug tolerant breast cancer cells. Indeed, we recently reported that EDCs such as bisphenol A and 2,2-bis(p-hydroxyphenyl)-1,1,1-trichloroethane upregulate epidermal growth factor receptor/extracellular signal-regulated kinase signaling and a corresponding increase in expression of SOD1 and antiapoptotic proteins leading to resistance to an epidermal growth factor receptor targeted drug (27).

While exposure to single EDCs and PAHs like bisphenol A and BaP have been studied extensively, it is crucial to note that rarely does single chemical exposure occur in the real world. Rather, humans are exposed to various chemicals in low doses, potentially resulting in cumulative toxic and carcinogenic effects. There remain difficulties in obtaining realistic and exposure-relevant chemical mixtures, including mixtures of PAHs, which provides a challenge for scientific discovery concerning the effects of mixture exposure.

In this study, sediment derived from the PAH-contaminated former United States Environmental Protection Agency (USEPA) Superfund site Atlantic Wood Industries (AWI) in Portsmouth, VA, along the Southern Branch of the Elizabeth River, provided an opportunity to derive a complex PAH mixture that represents a real-world exposure scenario. Pore-water extraction of Elizabeth River sediment at the AWI Superfund site followed by mass spectrometry characterization of PAH compounds in the resulting mixture revealed 36 known PAHs with concentrations ranging from 0.0003 to 0.341 ng/ml aqueous sediment extract, with naphthalene being the most highly concentrated (28,29). Previous studies have also shown the cancer and human exposure relevance of this mixture (30). This complex mixture provided us the perfect model EDC mixture for *in vitro* breast cancer cell exposure.

Our objective in this study was to determine if low-dose treatment with EDCs such as PAHs could not only upregulate AhR signaling in breast cancer cells but further cause an aggressive, hyperproliferative breast cancer phenotype. This is the first study to look at a naturally occurring PAH mixture with well-defined composition and identified doses that are relevant to human intake.

Methods

Human intake exposure analysis

Metabolite concentrations for four representative PAHs in the PAH mixture (naphthalene, fluorene, phenanthrene and pyrene) were obtained from the National Health and Nutrition Examination Survey (NHANES) database, years 2005–14. Excretion fractions of these PAHs in urine were obtained from the literature (31,32), as well as standardized daily adult urine output (33) and adult body weight (34). Using a back-of-the-envelope reverse dosimetry pharmacokinetic equation model described previously (35), we constructed estimated daily intake exposure for these four PAHs: exposure intake rate (μg/kg day) = [concentration$_{\text{urine metabolite}}$ × daily adult urine output × MW$_{\text{parent}}$]/[urinary excretion fraction × adult body weight × MW$_{\text{metabolite}}$]. These daily intake values were then compared with concentrations present in our complex PAH mixture diluents, based on mass spectrometry values shown in (30).

Toxic equivalence to benzo(*a*)pyrene for carcinogenicity

A toxic equivalence (TEQ) of the PAH mixture compared with B(*a*)P was completed using toxic equivalency fractions (TEFs) from the literature for 18 of the 36 compounds. A TEQ is calculated by multiplying the TEF for each compound by their concentration within the mixture, and summing the results to obtain a mixture TEQ.

Cell culture and reagents

Human mammary epithelial cells (HME1-tert), MCF-7 and MDA-MB-231 cells, both human breast adenocarcinoma cell lines, were obtained from the Duke University Cell Culture Facility. T47-D cells were a generous gift from the Blobe lab at Duke University. SUM149 cells, a human inflammatory breast cancer cell line, were obtained from Asterand, and all cell lines were cultured as per manufacturer's instructions and previous studies (36). Sediment extract containing the PAH mixture was prepared as described by Clark *et al.* (28) and stored in a glass container covered with aluminum foil at 4°C. BaP was purchased from Sigma–Aldrich and prepared in deionized water. Chlorothalonil, a potent fungicide shown to have cytotoxic effects in breast cancer cells (27), was obtained from Sigma–Aldrich. PAH mixture doses used in this study were 6, 30, 300 and 16 000 nM while BaP was used in 1 μM doses and chlorothalonil at a 5 μM dose. All cell lines were authenticated using short tandem repeat polymorphism analysis by the Duke DNA sequencing core prior to their use for this study, banked upon receipt and all cell lines were cultured for no more than 6 months during this study. Additionally, all cell lines used were short tandem repeat profiled within the past 6 months. All cell lines were cultured with 1% penicillin/streptomycin (Invitrogen) supplemented in their respective media. Cells were cultured in complete growth medium at 37°C under an atmosphere of 5% CO_2.

Ethoxyresorufin-O-deethylase activity analysis

Ethoxyresorufin-O-deethylase assay assesses cytochrome p450 (CYP1A1/CYP1B1) enzymatic activity. Cells were plated at 75 000 cells/well in 6-well plates and grown for 24 h, then treated as indicated. Twenty-four hours following treatment, cells were washed twice in Dulbecco's phosphate-buffered saline and incubated with 2 mM ethoxyresorufin in reaction buffer (50 mM Tris, 0.1 M NaCl, 6.23 mM $MgCl_2$, pH 7.8, warmed to 37°C). Then assay supernatant (100 μl) was transferred to a black-well clear bottom 96-well plate, and fluorescence was read in a BioTek© fluorescence plate reader at excitation λ (530 nm)/emission λ (590 nm). A resorufin standard curve was utilized from the same 96-well plate. Fluorescent counts were normalized to untreated cells.

Table 1. ER affinity and activity by individual PAH mixture parent, hydroxy, quinoid and ketone metabolite compounds

ER		Parent compound		Hydroxy metabolite(s)		Quinoid metabolite(s)		Ketone metabolite(s)		
PAH compound	Rings	Affinity	Activity	Affinity	Activity	Affinity	Activity	Affinity	Activity	References
Naphthalene	2		Weak inducer/ non-inducer		Inducer/ non-inducer	Binding	Non-inducer			(20,48,49,51,54)
Phenanthrene	3	Non-binding	Non-inducer	Binding	Inducer	Binding	Non-inducer			(20,48–52)
Fluoranthene	4	Non-binding	Non-inducer	Binding	Inducer					(20,50,51)
Acenaphthene	3	Non-binding/ weak binding	Non-inducer			Weak binding	Non-inducer			(20,48)
Fluorene	3	Non-binding	Non-inducer	Weak binding	Inducer/weak inducer			Weak binding	Non-inducer	(20,48,50–52,54)
Pyrene	4	Non-binding	Weak inducer/ non-inducer	Weak binding	Inducer/ non-inducer					(20,49–51,54)
Carbazole	3	Non-binding	Non-inducer							(52)
Dibenzofuran	3				Weak inducer					(54)
1-Methylnaphthalene	2		Inducer/ non-inducer							(20,54)
Benz[*a*]anthracene	4	Non-binding	Weak inducer	Binding	Inducer	Weak binding	Non-inducer	Weak binding	Non-inducer	(20,47,48,50–52,54)
Anthracene	3	Non-binding/ weak binding	Weak inducer/ non-inducer		Weak inducer	Binding/ weak binding	Weak inducer/ non-inducer	Weak binding	Non-inducer	(48,50,52,54)
Benzo[*b*]fluoranthene	5	Non-binding	Weak inducer/ non-inducer	Weak binding	Inducer	Weak binding	Non-inducer			(20,48,50,51,54)
Dibenzothiophene	3		Weak inducer/ non-inducer							(52)
Chrysene	4	Non-binding	Weak inducer/ non-inducer	Binding	Inducer/ non-inducer	Binding	Inducer			(20,47,48,50–52)
1,2-Benzofluorene/benzo(*a*) fluorene	4							Weak binding	Non-inducer	(48)
2,6-Dimethylnaphthalene	2		Weak inducer							(54)
BaP	5	Non-binding	Weak inducer/ non-inducer	Binding	Inducer/ non-inducer	Binding	Inducer	Non-binding	Non-inducer	(20,48,50–52,54)
Retene	3									
2-Methylphenanthrene	3		Non-inducer							(52)
Benzo[*e*]pyrene	5	Non-binding	Weak inducer/ non-inducer	Weak binding	Inducer					(50,51,54)
Benzo[*k*]fluoranthene	5	Non-binding	Weak inducer/ non-inducer	Binding	Inducer					(20,50,51,54)
1-Methylphenanthrene	3									
Acenaphthylene	3		Non-inducer							(20)
Benzo[*g*,*h*,*i*]perylene	6	Weak binding	Weak inducer/ non-inducer							(20,50,54)

Table 1. Continued

ER		Parent compound		Hydroxy metabolite(s)		Quinoid metabolite(s)		Ketone metabolite(s)		
PAH compound	Rings	Affinity	Activity	Affinity	Activity	Affinity	Activity	Affinity	Activity	References
Picene	5									
3,4-Benzofluorene/benzo(c) fluorene	4									
Perylene	5									
Benzo[a]fluoranthene	5									
Dibenz[a,l]pyrene	6									
Indeno[1,2,3-c,d]pyrene	6	Weak binding	Non-inducer		Non-inducer					(20,50,51)
Benzo[b]chrysene	5									
Dibenz[a,j]anthracene	5									
Dibenz[a,h]anthracene	5	Weak binding	Weak inducer/ non-inducer							(20,50,54)
Benzo[c]phenanthrene	4	Non-binding	Non-inducer	Binding	Weak inducer/ non-inducer	Binding				(47,48,51)
3-Methylcholanthrene	5	Weak binding	Weak inducer							(53,54)

For all 36 compounds within our Superfund sediment-derived PAH mixture, in order of descending mixture concentration. Affinity is defined by binding or displacement assay, to either the alpha or beta subunit of ER. Activity is defined by one or more of multiple assays: B-galactosidase activity, MVLN estrogen-responsive luciferase assay, estrogen responsive element fold induction in MCF-7 or other cell lines, or Yeast 2 Hybrid Assay. For some compounds, literature finds conflicting binding affinity or activity, and some compounds may exhibit antiestrogenic properties (data not shown). MVLN = also known as "MCF-7 Vit Luc Neo", a cell line based on MCF-7 that has been stably transfected so the luciferase gene is under the control of an estrogen-responsive element from the Xenopus vitellogenin A2 gene.

Cell proliferation assay

Cell proliferation were assessed by MTT assay (3-[4,5-dimethylthiazol-2-yl]-2,5-diphenyltetrazolium bromide), based on the conversion of MTT into formazan crystals by living cells, which determines metabolic activity and is an acceptable measure of viable, proliferating cells. Cells were seeded at 4000 cells/well into 96-well flat bottom plates. Cells were grown for 24 h then treated with PAH mixture (6, 30 or 300 nM), BaP (1 μM) or chlorothalonil (5 μM) then grown for another 24 h. Proliferation was assessed using 3(4,5-dimethylthiazol-2-yl)-2,5-diphenyltetrazolium, after which cells were incubated at 37°C for 2 h, dimethyl sulfoxide was added to each well and absorbance was read at 550 nm on a Molecular Devices plate reader.

Trypan blue exclusion viability assay

Cells were plated in a 12-well plate at 30 000 cells per well for 24 h, then treated with PAH mixture (6, 30, 300 or 16 000 nM), BaP (1 μM), chlorothalonil (5 μM) or left untreated. Cells were trypsinized after 24 h and resuspended in media, then centrifuged at 1600 rpm for 4 min. The supernatant was aspirated and 70 μl cold Dulbecco's phosphate-buffered saline added to the pellet. An aliquot of cell suspension was mixed with an equal volume of 0.4% trypan blue solution, and cell numbers were recorded in 10 μl of the resultant mixture using a hemocytometer.

Tumor organoid culture

SUM149 cell line was plated at 10 000 cells per well in an ultra-low attachment 24-well plate with filtered media supplemented with 2.25% polyethylene glycol as described previously (37,38). Organoids were left to form for 24 h, verified formed and uniform by microscopy, then treated with PAH mixture (6, 30, 300 and 16 000 nM), chlorothalonil (5 μM) or left untreated. Organoids were left to grow for 72 h on a rotating shaker at 40 rpm, after which they were imaged at ×4 magnification and their gross particle area was analyzed using NIH Image J.

Immunoblot analysis

Cells were seeded into 6-well plates at 75 000 cells/well and incubated for 24 h at 37°C, after which cells were treated with PAH mixture (6, 30 or 300 nM), BaP (1 μM) or left untreated then incubated for another 24 h. Alternatively, tumor organoids were treated as described above then left to grow for 72 h. Cells were then harvested and lysed after trypsinization, and immunoblot analysis was performed as described previously (25). Membranes were incubated overnight at 4°C with primary antibodies AhR, ER-a, SOD1, XIAP (1:1000 dilution) or glyceraldehyde 3-phosphate dehydrogenase (1:2000 dilution). Membranes were washed and incubated with anti-mouse or anti-rabbit horseradish peroxidase-conjugated antibodies (Cell Signaling Technologies) for 1 h at room temperature. Chemiluminescent substrate was applied for 5 min, and then membranes were exposed to radiographic film. Densitometric analysis was performed using NIH ImageJ software with glyceraldehyde 3-phosphate dehydrogenase as a loading control, where numbers represent analysis of total protein to glyceraldehyde 3-phosphate dehydrogenase, with all values normalized to the untreated lanes. Full immunoblot images can be found in Supplementary Material.

PAH ligand circuit mathematical model analysis

Simulations were performed in MATLAB (Mathworks) and bifurcation diagrams were drawn using MATCONT (39). The model formulation for the interactions among AhR, XIAP, nuclear factor-kappaB (NFκB) and CYP activity based on this study and published experimental work is given by:

$$\frac{dX}{dt} = g_X H^S(N, \lambda_{N,X}) H^S(E, \lambda_{E,X}) - k_X X$$

$$\frac{dN}{dt} = g_N H^S(X, \lambda_{X,N}) - k_N N$$

$$\frac{dA}{dt} = g_A H^S(P, \lambda_{P,A}) H^S(N, \lambda_{N,A}) H^S(A, \lambda_{A,A}) - k_A A$$

Table 2. AhR affinity and activity by individual PAH mixture parent, hydroxy, quinoid, and ketone metabolite compounds

AhR		Parent compound		Hydroxy metabolite(s)		Quinoid metabolite(s)		Ketone metabolite(s)		
PAH compound	Rings	Affinity	Activity	Affinity	Activity	Affinity	Activity	Affinity	Activity	References
Naphthalene	2		Weak inducer/ non-inducer		Inducer/weak inducer		Weak inducer			(20,58,60,61)
Phenanthrene	3	Binding	Weak inducer/ non-inducer				Non-inducer		Weak inducer	(20,55,56,58,60,61)
Fluoranthene	4		Weak inducer/ non-inducer							(20,58–60)
Acenaphthene	3		Weak inducer/ non-inducer							(20,58,60)
Fluorene	3		Weak inducer/ non-inducer		Inducer/weak inducer				Weak inducer	(20,57–61)
Pyrene	4		Weak inducer/ non-inducer		Weak inducer/ non-inducer					(20,58–61)
Carbazole	3		Weak inducer							(57)
Dibenzofuran	3				Inducer					(61)
1-Methylnaphthalene	2		Non-inducer							(20)
Benz[*a*]anthracene	4		Inducer/weak inducer				Inducer		Inducer	(20,57–60)
Anthracene	3		Weak inducer/ non-inducer		Inducer		Inducer/ weak inducer		Inducer	(20,57–61)
Benzo[*b*]fluoranthene	5	Binding	Inducer							(20,56,58–60)
Dibenzothiophene	3	Weak binding								(55)
Chrysene	4	Binding	Inducer/weak inducer		Weak inducer		Inducer		Inducer	(20,55,57–60)
1,2-Benzofluorene/benzo(*a*) fluorene	4								Inducer	(57,58)
2,6-Dimethylnaphthalene	2									
Benzo[*a*]pyrene	5		Inducer/weak inducer							(20,58–61)
Retene	3	Binding								(56)
2-Methylphenanthrene	3									
Benzo[*e*]pyrene	5		Weak inducer							(59)
Benzo[*k*]fluoranthene	5	Binding	Inducer							(20,58–60)
1-Methylphenanthrene	3	Weak binding								(56)
Acenaphthylene	3		Non-inducer							(20,58,60)
Benzo[*g*,*h*,*i*]perylene	6		Weak inducer/ non-inducer							(20,58–60)
Picene	5		Inducer							(59)
3,4-Benzofluorene/benzo(*c*) fluorene	4		Non-inducer						Inducer	(58,60)

Table 2. Continued

AhR		Parent compound		Hydroxy metabolite(s)		Quinoid metabolite(s)		Ketone metabolite(s)		
PAH compound	Rings	Affinity	Activity	Affinity	Activity	Affinity	Activity	Affinity	Activity	References
Perylene	5									
Benzo[*a*]fluoranthene	5									
Dibenz[*a*,*l*]pyrene	6		Weak inducer/ non-inducer							(59,60)
Indeno[1,2,3-*c*,*d*]pyrene	6		Inducer							(20,58–60)
Benzo[*b*]chrysene	5									
Dibenz[*a*,*j*]anthracene	5		Inducer							(59)
Dibenz[*a*,*h*]anthracene	5		Inducer							(20,58–60)
Benzo[*c*]phenanthrene	4		Weak inducer							(59)
3-Methylcholanthrene	5		Inducer							(58)

For all 36 compounds within our Superfund sediment-derived PAH mixture, in order of descending mixture concentration. Affinity is defined by TCDD displacement assay from AhR. Activity is defined by one or more of multiple assays, including luciferase assays, or induction equivalency factors for CYP1A1/CYP1B1 activity or equivalent activity compared to TCDD or BaP. AhR activity for many metabolite compounds not available in the literature, and some literature had conflicting conclusions as to AhR activity of certain PAH compounds. TCDD, 2,3,7,8-Tetrachlorodibenzodioxin.

where X, N and A denote the levels of XIAP, NFκB and AhR correspondingly, E represents an external signal that is increasing the levels of XIAP and P denotes PAH that are activating AhR. g_X, g_N and g_A represent their respective production rates, whereas k_X, k_N and k_A are respective degradation rates. $H^S(X, \lambda_{X,Y}) = H^-(X) + \lambda_{X,Y}(1 - H^-(X))$denote shifted Hill functions representing the effect of X on the production of Y, where $H^-(X)$ is the negative Hill function and $\lambda_{X,Y}$ represent the fold-change in the production of Y due to X. For inhibition, $\lambda_{X,Y} < 1$; for activation, $\lambda_{X,Y} > 1$, $\lambda_{X,Y} = 1$ denote no effect. $n_{X,Y}$ represents the strength of cooperativity of X in modulating Y. Degradation rates (represented in per hour) for XIAP, NFκB and AhR have been estimated based on experimental data on their half-lives (40–42). Production rate (denoted in molecules per hour) estimation is based on typical number of protein molecules reported for signaling molecules (~100 000) (43). Fold-change corresponding to the effect of XIAP on NFκB and vice versa was gathered from existing data (44–46), whereas that concerning the regulation of AhR has been estimated from our data. Bifurcation diagrams are drawn for the parameter E, for two different values of P = 0 (no exposure to PAH) and 500 (exposure to PAH).

Statistical analysis

Statistics were performed using the GraphPad InStat Student's two-tailed *t*-test or one-way analysis of variance with Fisher's least significant difference *post hoc* tests. Differences were considered significant at $P < 0.05$.

Results

PAH mixture is a complex, representative EDC mixture

As PAHs are a class of EDCs, we conducted a literature search to determine the estrogen receptor (ER alpha or beta) binding affinity and activity of the 36 individual components, as well as their related hydroxy, quinoid and ketone metabolite compounds (Table 1). Twenty-six PAH compounds (parent or metabolite) had adequate data on binding affinity or activity, although very few compounds had complete data (20,47–54) and nine compounds had no data available. No parent PAH compound was a strong inducer of ER activity or bound well to the receptor, but 11 hydroxy metabolites and 2 quinoid metabolites were inducers of ER activity as defined by the activity assays in each literature reference, not including weak inducers. Additionally, seven hydroxy metabolites and six quinoid metabolites exhibited significant ER binding. Ketone metabolites did not appear to be active. A few of the compounds and metabolites in the PAH mixture showed antiestrogenic activity in some induction assays, although these data are not shown due to inconsistent data and to maintain focus on positive estrogenic activity induction.

Next we queried for AhR activity and affinity (20,55–61) of the individual PAH compounds in the PAH mixture. Literature analysis identified five parent compounds with AhR strong binding affinity, while binding affinity data were not available for metabolites. In terms of AhR activity, most parent PAH compounds were weak inducers or non-inducers, and 10 compounds were potential inducers. Metabolites showed higher AhR activity capabilities, with four hydroxy metabolites, three quinoid metabolites and five ketone metabolites exhibiting activity induction, not including those which were weak inducers of AhR activity (Table 2).

Appreciating the PAH mixture complexity and potency of differing compounds, we conducted a literature search for PAH compound toxic equivalency factors (TEFs) and calculated a TEQ for carcinogenicity of the mixture using BaP as a reference (Supplementary Table 1, available at *Carcinogenesis* Online). TEFs were found for 18 of the 35 individual PAH compounds in the mixture (62,63). The mixture TEQ, which includes BaP as a component, was 251.77, while BaP alone within the mixture had a

TEF-concentration multiplier of 44.30. Notably within the mixture, dibenzo(*a*,*l*)pyrene, benzo(*b*)fluoranthene, fluoranthene, dibenz(*a*,*h*)anthracene and benz(*a*)anthracene dominated the TEQ, as these compounds had TEF-concentration multipliers of 62.00, 52.88, 33.81, 28.00 and 15.52, respectively. It is important to note that dibenzo(*a*,*l*)pyrene and dibenz(*a*,*h*)anthracene both had TEFs of 10, compared with BaP TEF of 1. These compounds had highly variable concentrations within the mixture, reflecting that the most highly concentrated components are not necessarily the most potent or cancer relevant, as can be expected from a highly complex chemical mixture.

Identifying low doses of the Superfund-derived PAH mixture relevant to human exposure

Although standard single PAH concentrations used for *in vitro* doses exist in the literature, to identify physiologically relevant doses, we used national urinary metabolite biomarker data from the NHANES survey years 2005–14 for four most abundant PAHs (naphthalene, fluorene, phenanthrene and pyrene) present in the Superfund-derived PAH mixture (28,29). A reverse dosimetry pharmacokinetic model was applied and when comparing these mean human exposures to compound concentrations present in the PAH mixture, the values were roughly equivalent and of the same order of magnitude as low nanomolar doses of 6 and 30 nM (Figure 1A). These concentrations along with a higher 300 nM treatment dose were subsequently used for the cell-based experiments in this study.

PAH mixture enhances proliferation of ER+ breast cancer cells through ER and AhR signaling

Based on the primary mechanism of PAH in inducing ER and AhR signaling and the link between ER and AhR activation (64), we investigated the Superfund-derived PAH-enriched mixture in MCF-7 (ER+) breast adenocarcinoma cells. Immunoblot data of PAH mixture treated cells at 24 h show increase in ER levels and AhR levels comparable to the cells treated with estrogen (E2) or the control PAH (BaP), respectively (Figure 1B and C). To further confirm AhR activation, we assessed ethoxyresorufin-*O*-deethylase activity, a sensitive and accurate bioassay in complex samples including breast cancer cells for determining CYP metabolic enzyme activity downstream of AhR, measuring both CYP1A1 and CYP1B1 activity together (65,66). There was a significant increase in CYP1A1/1B1 activity following 24 h treatment with PAH mixture (30 nM $P = 0.0147$, 300 nM $P = 0.0032$) or BaP treatment ($P < 0.0001$) (Figure 1D). Similar results with increasing AhR protein levels and CYP1A1/1B1 activity following low-dose treatment with PAH mixture for 24 h were observed in T47-D, another ER+ breast cancer cell line (Figure 1E and F).

This increase in AhR signaling in PAH treated cells corresponded with a significant increase in MCF-7 ER+ cell proliferation [PAH mixture 6, 30 and 300 nM all $P < 0.01$ or control 1 µM BaP ($P < 0.0001$)] compared with untreated cells (Figure 1G). In addition, none of the PAH mixture doses used, both low and high up to 16 µM, caused any changes in MCF-7 cell viability when compared with the cytotoxicity induced by 5 µM of chlorothalonil, a cytotoxic chemical control based on our previous studies (27) (Figure 1H).

We further tested the effect of the PAH mixture on viability, proliferation and AhR signaling in a panel of human breast cancer cell lines to represent diverse receptor subtypes. hTERT-HME1, an immortalized normal human mammary epithelial cell line (67), did not express significant levels of AhR and no induction or CYP activity was observed post PAH treatment (Figure 2A). In contrast to the ER+ MCF-7 and T47-D cells, treatment with similar doses of the single PAH BaP or the Superfund-derived PAH mixture in ER– breast cancer cells (MDA-MB-231 and SUM149, both triple negative breast carcinoma cell lines) did not cause any significant increase in AhR levels over basal expression, downstream CYP activity or changes in proliferation compared with untreated (Figure 2B and C).

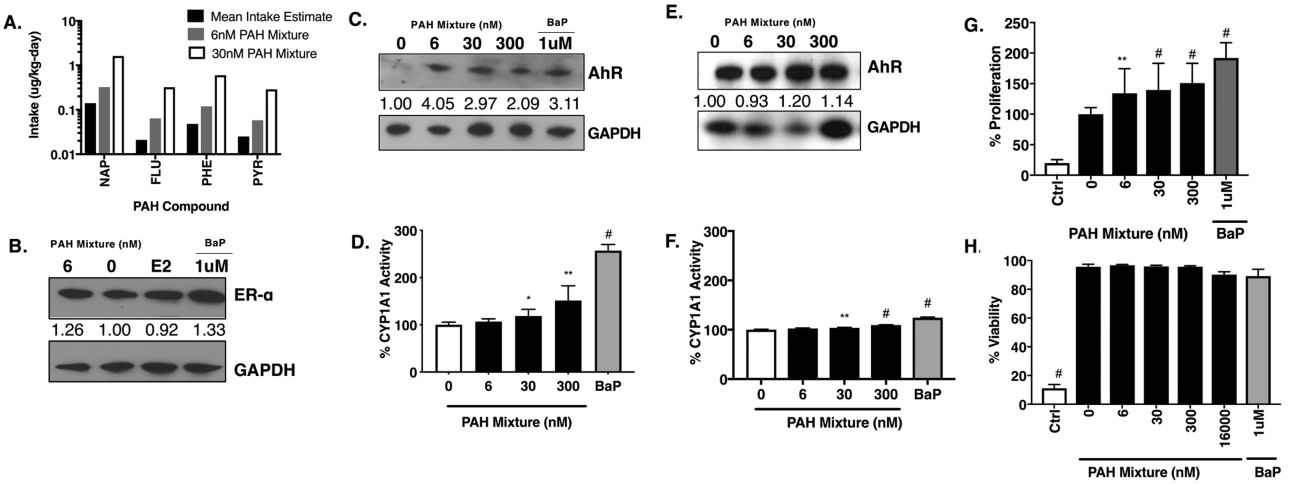

Figure 1. PAH mixture is non-toxic and upregulates AhR toxicant response pathway and 2D proliferation in ER+ breast cancer cells at doses relevant to human exposure. (**A**) Comparison of four PAH compound concentrations found in 6 and 30 nM doses of the PAH mixture with mean estimated intake of US adults for these same four PAH compounds. FLU, fluorine; NAP, naphthalene; PHE, phenanthrene; PYR, pyrene. (**B**) MCF-7 immunoblot and densitometry normalized to GAPDH and compared with untreated for ER-a following 24 h exposure to 6 nM PAH mixture, 1 µM BaP, estradiol (E2) or left untreated. (**C** and **D**) Cropped immunoblot of the AhR with densitometry values normalized to GAPDH and compared with untreated and downstream CYP1A1/CYP1B1 enzyme activity by ethoxyresorufin-*O*-deethylase assay analysis in MCF-7 cells and (**E** and **F**) T47-D cells following 24 h PAH mixture treatment. AhR (100 kD), aryl hydrocarbon receptor; GAPDH (36 kD), glyceraldehyde 3-phosphate dehydrogenase. (**G**) Proliferation by MTT assay and (**H**) viability count in MCF-7 cells following low-dose PAH mixture or 1 µM BaP single chemical treatment for 24 h. BaP, benzo(*a*)pyrene; Ctrl, 5 µM chlorothalonil cytotoxic chemical control. $^{*}P < 0.05$, $^{**}P < 0.01$, $^{***}P < 0.001$, $^{\#}P < 0.0001$.

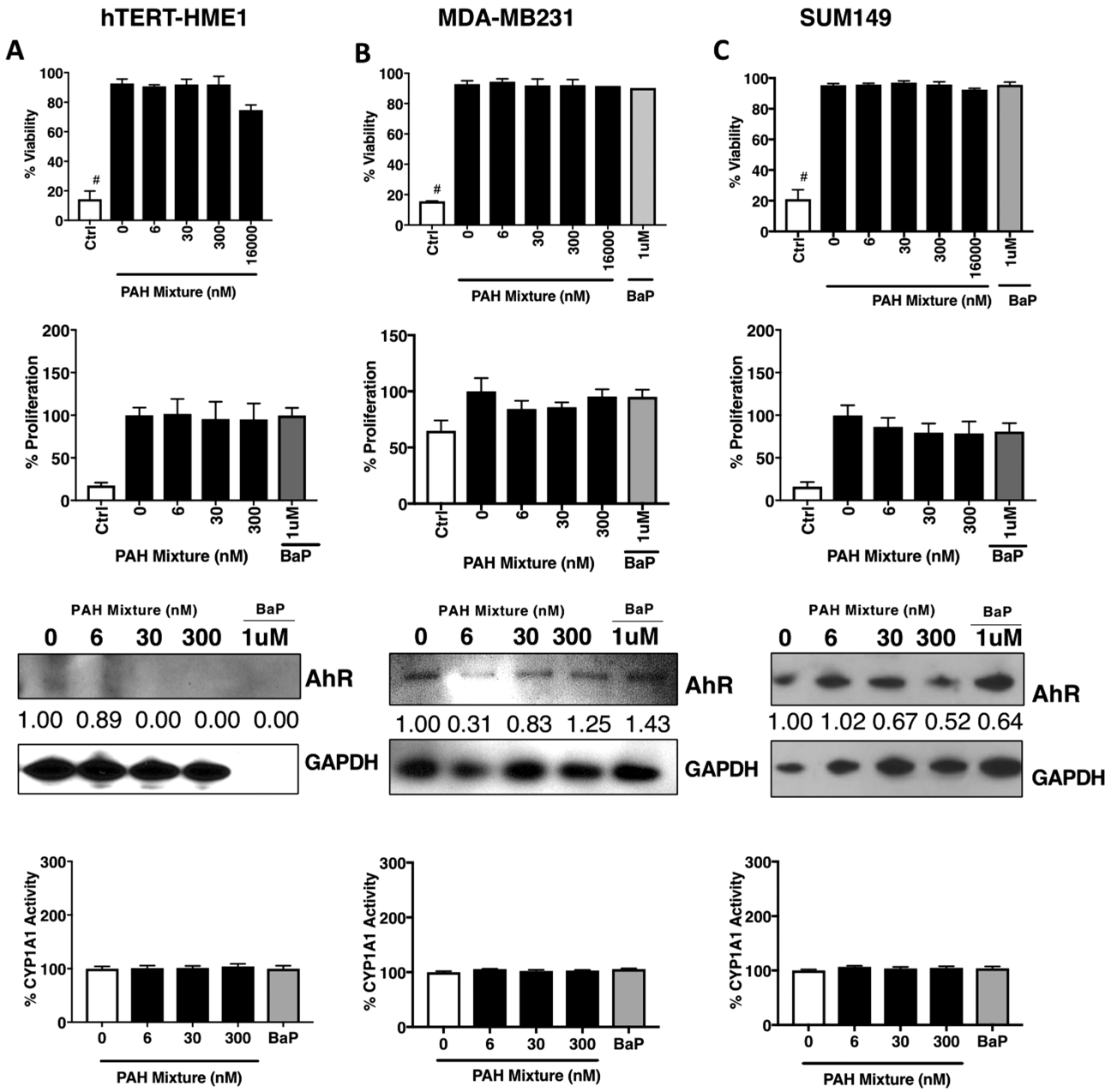

Figure 2. Treatment with low-dose PAH mixture does not affect viability, proliferation or the AhR toxicant response pathway in normal mammary or ER– breast cancer cells. For (**A**) hTERT-HME1 normal human mammary, (**B**) MDA-MB231 triple negative and (**C**) SUM149 triple negative breast cancer cells: Viability counts following low-dose PAH mixture or 1 μM BaP single chemical treatment for 24 h. BaP, benzo(*a*)pyrene; Ctrl, 5 μM chlorothalonil cytotoxic chemical control. $^{\#}P < 0.0001$. Proliferation by MTT assay following low-dose PAH mixture or 1 μM BaP single chemical treatment for 24 h. Cropped immunoblot of the AhR with densitometry values normalized to GAPDH and compared with untreated. AhR (100 kD), aryl hydrocarbon receptor; GAPDH (36 kD), glyceraldehyde 3-phosphate dehydrogenase. CYP1A1/CYP1B1 enzyme activity by ethoxyresorufin-O-deethylase assay analysis in following 24 h PAH mixture treatment or treatment with 1 μM BaP single chemical.

Low-dose PAH mixture enhances tumor emboli/organoid growth

Recently, we reported (38) differential effects of targeting survival signaling in SUM149, a highly heterogenous cell line derived from a primary, untreated, inflammatory breast cancer patient tumor, when grown as 3D cultures compared with 2D conditions (38). Using this 3D simulation model (37,38), wherein tumors cells are induced to form tumor cell emboli/organoids similar to the clinicopathological hallmark observed in inflammatory breast cancer patients, we tested the effects of the PAH mixture (Figure 3A). Although SUM149 2D cultures were inert to PAH exposure (Figure 2C), a significant increase in 3D tumor organoid area with PAH mixture treatment at 30 and 300 nM and toxicity at higher 16 000 nM dose or when exposed to the cytotoxic chemical (5 μM chlorothalonil) (Figure 3B and C) was observed. Additionally, these organoids sustained both antioxidant SOD1 and antiapoptotic XIAP survival signaling protein levels in addition to mitogen-activated protein kinase proliferative pathway extracellular signal-regulated kinase protein levels at low-dose PAH mixture exposure (Figure 3D).

Low-dose PAH mixture increases stress response-mediated tumor cell survival signaling

In order to test the hypothesis that environmental chemicals act as cellular stressors and activate survival signaling in

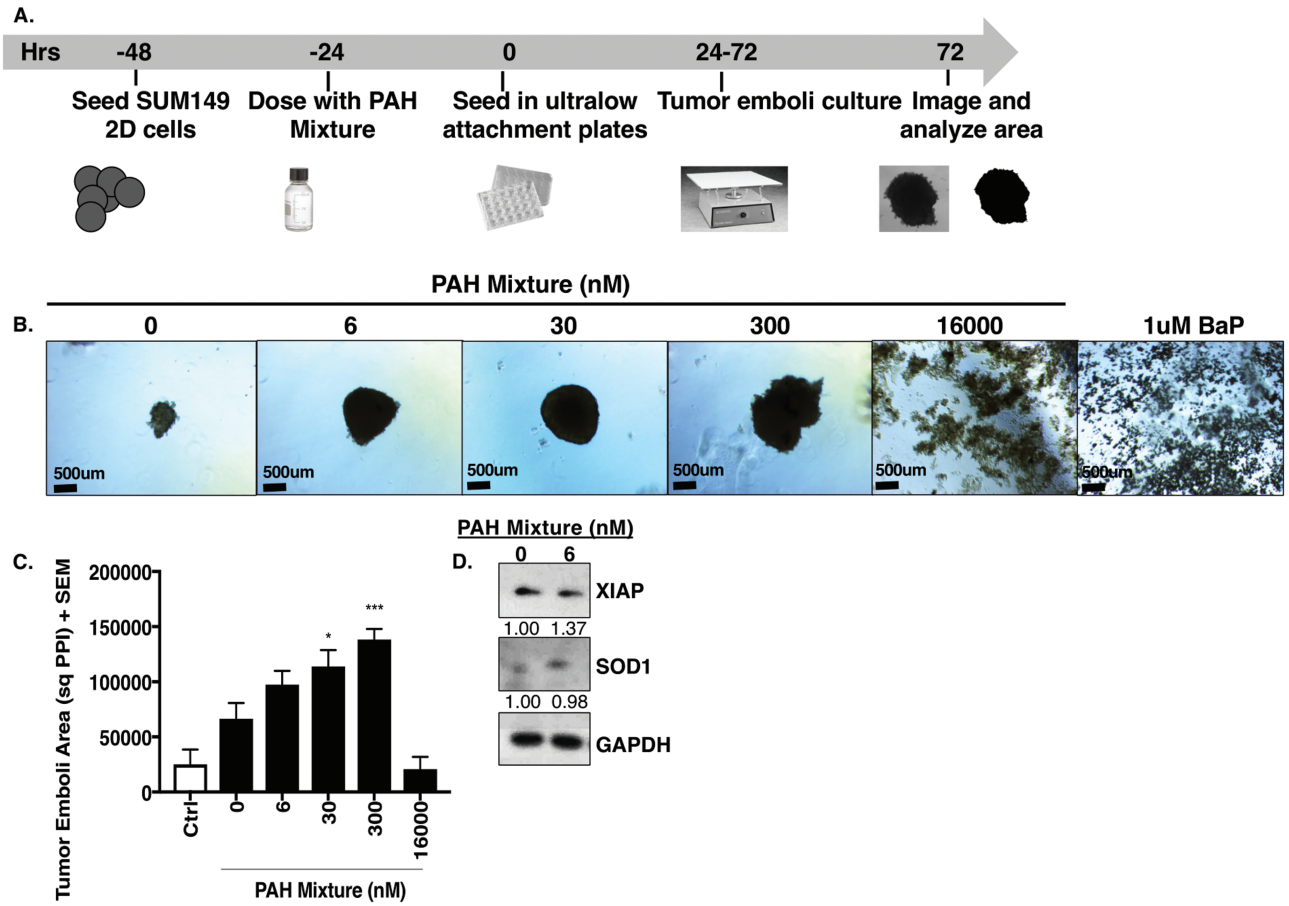

Figure 3. Treatment with low-dose PAH mixture exacerbates aggressive triple negative tumor organoid formation. (**A**) Schema of tumor organoid growth assay. (**B**) Representative images, (**C**) area quantification and (**D**) western immunoblots for XIAP and SOD1 with densitometry values normalized to GAPDH of SUM149 inflammatory breast cancer cell line 3D organoids treated with PAH mixture for 72 h. Scale bar = 500 μm. BaP, benzo(*a*)pyrene; Ctrl, 5 μM chlorothalonil cytotoxic chemical control; GAPDH (36 kD), glyceraldehyde 3-phosphate dehydrogenase; SOD1 (23 kD), superoxide dismutase; XIAP (53 kD), X-linked inhibitor of apoptosis protein. $^{*}P < 0.05$, $^{***}P < 0.001$.

tumor cells to adapt and overcome stress-mediated cell death stimuli, we assessed the PAH mixture treated cells for markers of an adaptive stress response signaling pathway. We have recently (68) reported a dominant role of X-linked inhibitor of apoptosis protein (XIAP, potent antiapoptotic protein and regulator of nuclear transcription factor NFκB and its target genes like SOD1) in enhancing aggressive breast cancer tumor growth and hyperproliferative phenotype (36,69,70). Indeed, PAH mixture treatment caused upregulation of XIAP and SOD1 proteins (Figure 4A and B) in ER+ MCF-7 and T47-D breast cancer cell lines.

Integrating our abovementioned quantitative signaling data following PAH exposure with earlier reports indicating crosstalk between XIAP and NFκB pathways (44,45) and transcriptional activation of AhR by NFκB (46), we constructed a mathematical model to predict the dynamics of PAH exposure and survival signaling in MCF-7 ER+ cells. The model predicts that even without PAH treatment, the system is bistable, i.e. cells can exist in a high XIAP/high NFκB/high AhR or a low XIAP/low NFκB/low AhR state. However, upon PAH treatment, two key changes are observed. First, intrinsic levels of AhR increase approximately twice (compare the lower green branch versus lower blue branch). Second, PAH treatment stabilizes the high XIAP/high NFκB/high AhR state; the difference in AhR levels between the two states is higher upon exposure to PAH as compared with that when the cells are not exposed to PAH, thereby making the transition from high XIAP/high NFκB/high AhR to low XIAP/low NFκB/low AhR state even more difficult (compare the length of dotted black arrows between green curves and those between blue curves in middle) (Figure 4C). Based on the aforementioned signaling and mathematical model datasets, a schema of the signaling implications of PAH mixture treatment on activation of AhR and ER, and upregulation of AhR responsive proteins CYP1A1/CYP1B1, SOD1 and antiapoptotic XIAP in ER+ cells is shown in Figure 4D.

Discussion

Elucidating the impact of complex chemical mixtures in our environment, in particular those identified as carcinogens of concern, is of significant interest in tumor biology and therapeutic outcomes. This study investigated, and to our knowledge is the first to report, the mitogenic signaling effects of a pore-water extract from the river sediments of a Superfund site in normal, ER+ and ER– breast cancer cells. Our previous studies revealed that this sediment extract is enriched with PAHs, in particular 36 separate PAH compounds detected using mass spectrometry (28,29), many of which also have potential carcinogenic properties (30). Herein, using previously published datasets, we first determined that the Superfund-derived extract is representative of a complex endocrine-disrupting mixture of compounds, which can potentially perturb ER and AhR pathway signaling.

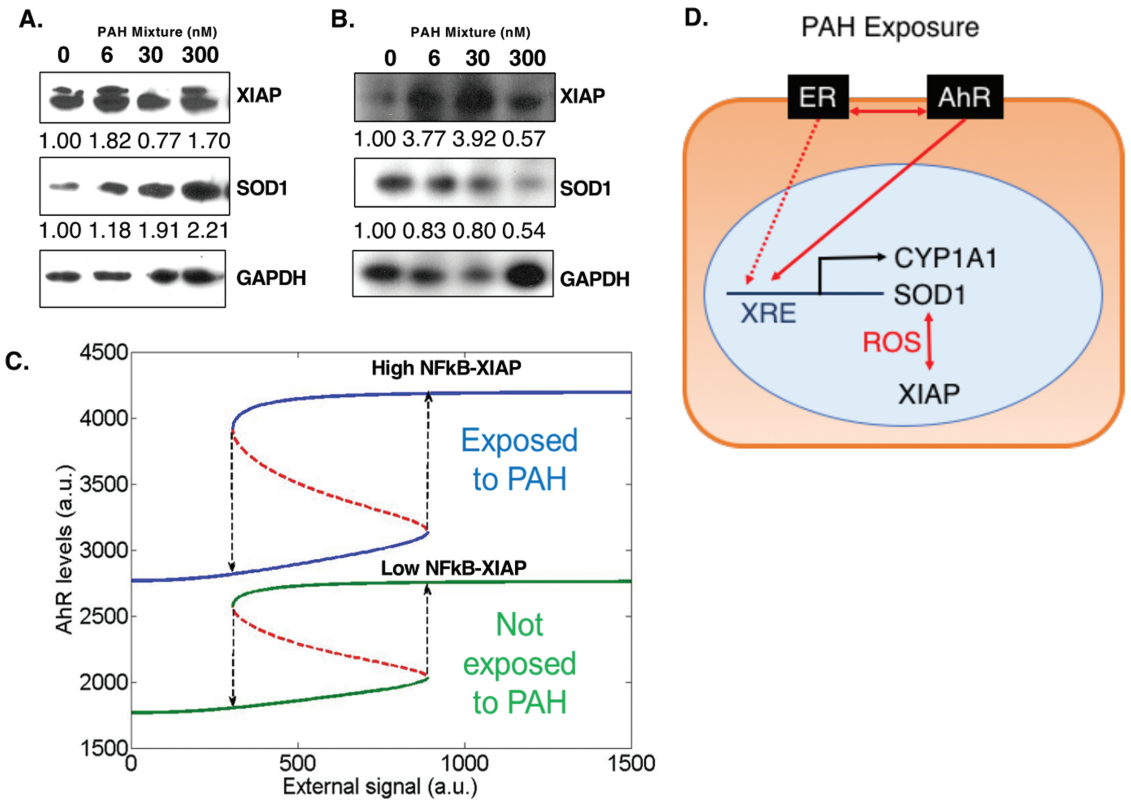

Figure 4. Treatment with low-dose PAH mixture increases survival signaling in ER+ breast cancer cells stabilized by high XIAP levels. (**A**) Cropped immunoblots with densitometry values normalized to GAPDH and compared with untreated cells for XIAP and SOD1 for (A) MCF-7 and (**B**) T47-D cells following 24 h treatment with low-dose PAH mixture. GAPDH (36 kD), glyceraldehyde 3-phosphate dehydrogenase; SOD1 (23 kD), superoxide dismutase; XIAP (53 kD), X-linked inhibitor of apoptosis protein. (**C**) Bifurcation diagram showing how cells can switch back and forth between high AhR and low AhR states. Solid lines represent stable states, dotted red lines unstable steady states. Blue curve represents the case when cells are treated with PAH, green curve denotes the case when cells are not treated with PAH. (**D**) Classic toxicant and oncogenic pathways affected by our low-dose PAH mixture treatment, allowing for increased cancer cell proliferation and survival.

The estrogenic activity seemed largely due to the result of metabolites, hydroxy, quinoid or ketone derivatives of its PAH components consistent with previous reports (20,47–54). We also determined that the mixture has high potential toxicity, with a TEQ much higher than that of BaP alone, a potent carcinogen on its own.

To identify physiologically relevant concentrations of the PAH mixture for cell-based studies, we first conducted reverse dosimetry modeling to determine mean US adult exposure to four select PAHs in the sediment extract. Only four PAH urinary metabolites—naphthalene, fluorene, phenanthrene and pyrene—are available in this database, however, all four are on the USEPA list of priority PAHs due to their potential carcinogenic concern (71), and all are present at high concentrations in the sediment extract. Additionally, urinary metabolites are an accepted and previously used method by which to estimate exposure to PAHs (72–74). Based on the calculated estimates of exposure, we selected 6, 30 and 300 nM of PAH mixture as representative low doses (6 nM doses relevant to average exposure, while 30 and 300 nM are more pertinent to vulnerable subpopulations exposed to potential higher PAH exposure conditions).

The impacts of individual PAH chemical exposures in breast cancer cells, including MCF-7, have been well studied (75–77). However, the effects of a well-characterized complex PAH mixture relevant to human exposure in cancer models is lacking. Therefore, our observations that the Superfund-derived mixture with known PAH components causes upregulation of ER levels, AhR activity and downstream increase in antiapoptotic and antioxidant proteins in ER+ cells and enhances a proliferative phenotype in both ER+ and ER– cells (tumor organoid growth) is of significance. The ability of AhR to recruit ER to AhR-regulated genes has been previously described, as well as the ability of AhR to control ER signaling (78–80). This modulation includes recruitment of ER to AhR growth factor targets, which we speculate may reinforce any proliferative abilities of the PAH compounds in the mixture. Recently, we reported the mitogenic effect of EDCs like bisphenol A, as single agents, in increasing breast cancer proliferation and therapeutic resistance (27).

AhR has also been found to be constitutively active in many cancers (81), including aggressive breast cancers (82,83), in contrast to insignificant levels found in normal breast cells like HME1 (67) used in the current study wherein the PAH treatments had no effects. A mathematical model was constructed representing the relationship between PAH ligand and AhR and including the relationship between XIAP and master transcriptional regulator NFκB. This model showed that PAH chemical presence in the cellular system leads to more stable and higher AhR and XIAP levels. This model incorporated data from MCF-7 ER+ cells, and further contributes to the possibility of upregulated survival and stress response signaling via XIAP as mechanisms of cell survival in ER+ breast cancer cells. Taken together, these results demonstrate that a complex PAH mixture, representing a model class of environmental chemicals, has the potential to induce and stabilize/maintain a hyperproliferative cellular phenotype characterized by

enhanced AhR, and XIAP-mediated stress response survival signaling.

Supplementary material

Supplementary data are available at *Carcinogenesis* online.

Funding

This work was supported in part by developmental funds from the Duke Cancer Institute/DCI P3917733 and P30CA014236 (GRD), a pilot grant from DCI Cancer and Environment Program (GRD), Department of Surgery Bolognesi award (GRD), training grant National Institute for Environmental Health Sciences T32-ES021432 (LMGS), National Cancer Institute training grant T32CA009111 (SJS), training fellowship from the Gulf Coast Consortia on the Computational Cancer Biology Training Program (Cancer Prevention and Research Institute grant no. RP170593) (MKJ) and a Duke Trinity College of Arts and Sciences Undergraduate Research Support (URS) award (JBD).

Acknowledgements

We thank Moises Tacam Jr for his help in the exposure analysis, and Devi lab members for their input in project discussions.
Conflict of Interest Statement: None declared.

Authors' contribution

GRD and RDG conceptualized the project; GRD, JBD, SJS, NJ and LMGS designed experiments; LMGS, JBD and SJS conducted experiments; LMGS, JBD, SJS, NJ, RDG, MKJ and GRD analyzed, interpreted and approved the manuscript; MKJ developed the mathematical model; LMGS, JBD and GRD wrote the manuscript; GRD and RDG mentored and provided oversight throughout the project.

References

1. American Cancer Society (2017) *Breast Cancer Facts & Figures 2017–2018*. American Cancer Society, Atlanta, GA.
2. Carter, C.L. *et al.* (1989) Relation of tumor size, lymph node status, and survival in 24,740 breast cancer cases. *Cancer*, 63, 181–187.
3. Brandt, J. *et al.* (2015) Age at diagnosis in relation to survival following breast cancer: a cohort study. *World J. Surg. Oncol.*, 13, 33.
4. Shulman, L.N. *et al.* (2010) Breast cancer in developing countries: opportunities for improved survival. *J. Oncol.*, 2010, 595167.
5. Soerjomataram, I. *et al.* (2008) An overview of prognostic factors for long-term survivors of breast cancer. *Breast Cancer Res. Treat.*, 107, 309–330.
6. Giulivo, M. *et al.* (2016) Human exposure to endocrine disrupting compounds: their role in reproductive systems, metabolic syndrome and breast cancer. A review. *Environ. Res.*, 151, 251–264.
7. Soto, A.M. *et al.* (2010) Environmental causes of cancer: endocrine disruptors as carcinogens. *Nat. Rev. Endocrinol.*, 6, 363–370.
8. Birnbaum, L.S. *et al.* (2003) Cancer and developmental exposure to endocrine disruptors. *Environ. Health Perspect.*, 111, 389–394.
9. Fenton, S.E. (2006) Endocrine-disrupting compounds and mammary gland development: early exposure and later life consequences. *Endocrinology*, 147(6 suppl.), S18–S24.
10. Snedeker, S.M. (2001) Pesticides and breast cancer risk: a review of DDT, DDE, and dieldrin. *Environ. Health Perspect.*, 109 (suppl. 1), 35–47.
11. Gore, A.C. *et al.* (2015) Executive summary to EDC-2: the endocrine society's second scientific statement on endocrine-disrupting chemicals. *Endocr. Rev.*, 36, 593–602.
12. Lioy, P.J. *et al.* (2011) Exposure science and the exposome: an opportunity for coherence in the environmental health sciences. *Environ. Health Perspect.*, 119, A466–A467.
13. Miller, G.W. *et al.* (2014) The nature of nurture: refining the definition of the exposome. *Toxicol. Sci.*, 137, 1–2.
14. Rappaport, S.M. (2013) What is the exposome. *Cancer*, 22.
15. US Environmental Protection Agency (2014) *Endocrine Disruptor Screening Program Universe of Chemicals and General Validation Principles*. http://www.epa.gov/endo/index.htm#universe (7 January 2019, date last accessed).
16. Interagency Breast Cancer and Environmental Research Coordinating Committee (2013) *Breast Cancer and the Environment: Prioritizing Prevention*. National Institutes of Health, Bethesda, MD.
17. Ramesh, A. *et al.* (2011) Global environmental distribution and human health effects of polycyclic aromatic hydrocarbons. In *Global Contamination Trends of Persistent Organic Chemicals*. pp. 95–124.
18. Large, C. *et al.* (2017) Geographic variations in female breast cancer incidence in relation to ambient air emissions of polycyclic aromatic hydrocarbons. *Environ. Sci. Pollut. Res. Int.*, 24, 17874–17880.
19. Shen, J. *et al.* (2017) Dependence of cancer risk from environmental exposures on underlying genetic susceptibility: an illustration with polycyclic aromatic hydrocarbons and breast cancer. *Br. J. Cancer*, 116, 1229–1233.
20. Villeneuve, D.L. *et al.* (2002) Relative potencies of individual polycyclic aromatic hydrocarbons to induce dioxinlike and estrogenic responses in three cell lines. *Environ. Toxicol.*, 17, 128–137.
21. Mahadevan, B. *et al.* (2007) Competitive inhibition of carcinogen-activating CYP1A1 and CYP1B1 enzymes by a standardized complex mixture of PAH extracted from coal tar. *Int. J. Cancer*, 120, 1161–1168.
22. Angus, W.G. *et al.* (1999) Expression of CYP1A1 and CYP1B1 depends on cell-specific factors in human breast cancer cell lines: role of estrogen receptor status. *Carcinogenesis*, 20, 947–955.
23. Savas, U. *et al.* (1997) Biological oxidations and P450 reactions. Recombinant mouse CYP1B1 expressed in *Escherichia coli* exhibits selective binding by polycyclic hydrocarbons and metabolism which parallels C3H10T1/2 cell microsomes, but differs from human recombinant CYP1B1. *Arch. Biochem. Biophys.*, 347, 181–192.
24. Burdick, A.D. *et al.* (2003) Benzo(a)pyrene quinones increase cell proliferation, generate reactive oxygen species, and transactivate the epidermal growth factor receptor in breast epithelial cells. *Cancer Res.*, 63, 7825–7833.
25. Aird, K.M. *et al.* (2012) ErbB1/2 tyrosine kinase inhibitor mediates oxidative stress-induced apoptosis in inflammatory breast cancer cells. *Breast Cancer Res. Treat.*, 132, 109–119.
26. Williams, K.P. *et al.* (2013) Quantitative high-throughput efficacy profiling of approved oncology drugs in inflammatory breast cancer models of acquired drug resistance and re-sensitization. *Cancer Lett.*, 337, 77–89.
27. Sauer, S.J. *et al.* (2017) Bisphenol A activates EGFR and ERK promoting proliferation, tumor spheroid formation and resistance to EGFR pathway inhibition in estrogen receptor-negative inflammatory breast cancer cells. *Carcinogenesis*, 38, 252–260.
28. Clark, B.W. *et al.* (2013) Compound- and mixture-specific differences in resistance to polycyclic aromatic hydrocarbons and PCB-126 among Fundulus heteroclitus subpopulations throughout the Elizabeth River estuary (Virginia, USA). *Environ. Sci. Technol.*, 47, 10556–10566.
29. Fang, M. *et al.* (2014) Effect-directed analysis of Elizabeth River porewater: developmental toxicity in zebrafish (*Danio rerio*). *Environ. Toxicol. Chem.*, 33, 2767–2774.
30. Gearhart-Serna, L.M. *et al.* (2018) Assessing cancer risk associated with aquatic polycyclic aromatic hydrocarbon pollution reveals dietary routes of exposure and vulnerable populations. *J. Environ. Public Health*, 2018, 5610462.
31. Li, Z. *et al.* (2012) Excretion profiles and half-lives of ten urinary polycyclic aromatic hydrocarbon metabolites after dietary exposure. *Chem. Res. Toxicol.*, 25, 1452–1461.
32. El-Masri, H. (2005) *Toxicological Profile for Naphthalene, 1-Methylnaphthalene, and 2-Methylnaphthalene*. US Department of Health and Human Services, Agency for Toxic Substances and Disease Registry.
33. Addis, T. (1923) The clinical significance of abnormalities in urine volumes. *Arch. Intern. Med.*, 31, 783–796.
34. Moya, J. *et al.* (2011). *Exposure Factors Handbook: 2011 edition*. US Environmental Protection Agency.

35. Hoffman, K. *et al.* (2017) Estimated tris(1,3-dichloro-2-propyl) phosphate exposure levels for US infants suggest potential health risks. *Environ. Sci. Technol. Lett.*, 4, 334–338.
36. Allensworth, J.L. *et al.* (2012) XIAP inhibition and generation of reactive oxygen species enhances TRAIL sensitivity in inflammatory breast cancer cells. *Mol. Cancer Ther.*, 11, 1518–1527.
37. Arora, J. *et al.* (2017) Inflammatory breast cancer tumor emboli express high levels of anti-apoptotic proteins: use of a quantitative high content and high-throughput 3D IBC spheroid assay to identify targeting strategies. *Oncotarget*, 8, 25848–25863.
38. Bocci, F. *et al.* (2019) Toward understanding cancer stem cell heterogeneity in the tumor microenvironment. *Proc. Natl. Acad. Sci. USA*, 116, 148–157.
39. Dhooge, A. *et al.* (2003) MATCONT: a MATLAB package for numerical bifurcation analysis of ODEs. *ACM Trans. Math. Softw. (TOMS)*, 29, 141–164.
40. Gu, L. *et al.* (2009) Regulation of XIAP translation and induction by MDM2 following irradiation. *Cancer Cell*, 15, 363–375.
41. Lipniacki, T. *et al.* (2004) Mathematical model of NF-kappaB regulatory module. *J. Theor. Biol.*, 228, 195–215.
42. Swanson, H.I. *et al.* (1993) Half-life of aryl hydrocarbon receptor in Hepa 1 cells: evidence for ligand-dependent alterations in cytosolic receptor levels. *Arch. Biochem. Biophys.*, 302, 167–174.
43. Milo, R. *et al.* (2010) BioNumbers—the database of key numbers in molecular and cell biology. *Nucleic Acids Res.*, 38(Database issue), D750–D753.
44. Lu, M. *et al.* (2007) XIAP induces NF-kappaB activation via the BIR1/TAB1 interaction and BIR1 dimerization. *Mol. Cell*, 26, 689–702.
45. Lin, M.T. *et al.* (2004) Cyr61 expression confers resistance to apoptosis in breast cancer MCF-7 cells by a mechanism of NF-kappaB dependent XIAP up-regulation. *J. Biol. Chem.*, 279, 24015–24023.
46. Vogel, C.F. *et al.* (2014) Cross-talk between aryl hydrocarbon receptor and the inflammatory response a role for nuclear factor-κB. *J. Biol. Chem.*, 289:1866–1875.
47. Fertuck, K.C. *et al.* (2001) Interaction of PAH-related compounds with the alpha and beta isoforms of the estrogen receptor. *Toxicol. Lett.*, 121, 167–177.
48. Hayakawa, K. *et al.* (2011) Estrogenic/antiestrogenic activities of quinoid polycyclic aromatic hydrocarbons. *J. Health Sci.* 57, 274–280.
49. Sievers, C.K. *et al.* (2013) Differential action of monohydroxylated polycyclic aromatic hydrocarbons with estrogen receptors α and β. *Toxicol. Sci.*, 132, 359–367.
50. Gozgit, J.M. *et al.* (2004) Differential action of polycyclic aromatic hydrocarbons on endogenous estrogen-responsive genes and on a transfected estrogen-responsive reporter in MCF-7 cells. *Toxicol. Appl. Pharmacol.*, 196, 58–67.
51. Hayakawa, K. *et al.* (2007) Estrogenic/antiestrogenic activities of polycyclic aromatic hydrocarbons and their monohydroxylated derivatives by yeast two-hybrid assay. *J. Health Sci.*, 53, 562–570.
52. Lam, M.M. *et al.* (2018) Methylated polycyclic aromatic hydrocarbons and/or their metabolites are important contributors to the overall estrogenic activity of polycyclic aromatic hydrocarbon-contaminated soils. *Environ. Toxicol. Chem.*, 37, 385–397.
53. Abdelrahim, M. *et al.* (2006) 3-Methylcholanthrene and other aryl hydrocarbon receptor agonists directly activate estrogen receptor alpha. *Cancer Res.*, 66, 2459–2467.
54. Nishihara, T. *et al.* (2000) Estrogenic activities of 517 chemicals by yeast two-hybrid assay. *J. Health Sci.*, 46, 282–298.
55. Lee, S. *et al.* (2015) Measured and predicted affinities of binding and relative potencies to activate the AhR of PAHs and their alkylated analogues. *Chemosphere*, 139, 23–29.
56. Billiard, S.M. *et al.* (2002) Binding of polycyclic aromatic hydrocarbons (PAHs) to teleost aryl hydrocarbon receptors (AHRs). *Comp. Biochem. Physiol. B: Biochem. Mol. Biol.*, 133, 55–68.
57. Larsson, M. *et al.* (2014) Time-dependent relative potency factors for polycyclic aromatic hydrocarbons and their derivatives in the H4IIE-luc bioassay. *Environ. Toxicol. Chem.*, 33, 943–953.
58. Misaki, K. *et al.* (2007) Aryl hydrocarbon receptor ligand activity of polycyclic aromatic ketones and polycyclic aromatic quinones. *Environ. Toxicol. Chem.*, 26, 1370–1379.
59. Machala, M. *et al.* (2001) Aryl hydrocarbon receptor-mediated activity of mutagenic polycyclic aromatic hydrocarbons determined using *in vitro* reporter gene assay. *Mutat. Res.*, 497, 49–62.
60. Pieterse, B. *et al.* (2013) PAH-CALUX, an optimized bioassay for AhR-mediated hazard identification of polycyclic aromatic hydrocarbons (PAHs) as individual compounds and in complex mixtures. *Environ. Sci. Technol.*, 47, 11651–11659.
61. Ohura, T. *et al.* (2010) Aryl hydrocarbon receptor activities of hydroxylated polycyclic aromatic hydrocarbons in recombinant yeast cells. *Toxicol. Environ. Chem.*, 92, 737–742.
62. Nisbet, I.C. *et al.* (1992) Toxic equivalency factors (TEFs) for polycyclic aromatic hydrocarbons (PAHs). *Regul. Toxicol. Pharmacol.*, 16, 290–300.
63. Andersson, J.T. *et al.* (2015) Time to say goodbye to the 16 EPA PAHs? Toward an up-to-date use of PACs for environmental purposes. *Polycycl. Aromat. Compd.*, 35, 330–354.
64. Ohtake, F. *et al.* (2003) Modulation of oestrogen receptor signalling by association with the activated dioxin receptor. *Nature*, 423, 545–550.
65. Divi, R.L. *et al.* (2014) Correlation between CYP1A1 transcript, protein level, enzyme activity and DNA adduct formation in normal human mammary epithelial cell strains exposed to benzo[a]pyrene. *Mutagenesis*, 29, 409–417.
66. Heger, S. *et al.* (2016) Microscale *in vitro* assays for the investigation of neutral red retention and ethoxyresorufin-O-deethylase of biofuels and fossil fuels. *PLoS One*, 11, e0163862.
67. Brooks, J. *et al.* (2011) Malignant transformation of mammary epithelial cells by ectopic overexpression of the aryl hydrocarbon receptor. *Curr. Cancer Drug Targets*, 11, 654–669.
68. Evans, M.K. *et al.* (2018) XIAP regulation by MNK links MAPK and NFκB signaling to determine an aggressive breast cancer phenotype. *Cancer Res.*, 78(7), 1726–1738.
69. Allensworth, J.L. *et al.* (2015) Disulfiram (DSF) acts as a copper ionophore to induce copper-dependent oxidative stress and mediate anti-tumor efficacy in inflammatory breast cancer. *Mol. Oncol.*, 9, 1155–1168.
70. Evans, M.K. *et al.* (2016) X-linked inhibitor of apoptosis protein mediates tumor cell resistance to antibody-dependent cellular cytotoxicity. *Cell Death Dis.*, 7, e2073.
71. U.S. Environmental Protection Agency (1982) *EPA Method 610: Polynuclear Aromatic Hydrocarbons*. US Environmental Protection Agency.
72. Strickland, P. *et al.* (1996) Polycyclic aromatic hydrocarbon metabolites in urine as biomarkers of exposure and effect. *Environ. Health Perspect.*, 104 (suppl. 5), 927–932.
73. Strickland, P. *et al.* (1999) Urinary 1-hydroxypyrene and other PAH metabolites as biomarkers of exposure to environmental PAH in air particulate matter. *Toxicol. Lett.*, 108, 191–199.
74. Fillmann, G. *et al.* (2004) Urinary PAH metabolites as biomarkers of exposure in aquatic environments. *Environ. Sci. Technol.*, 38, 2649–2656.
75. Korsh, J. *et al.* (2015) Polycyclic aromatic hydrocarbons and breast cancer: a review of the literature. *Breast Care (Basel)*, 10, 316–318.
76. Plísková, M. *et al.* (2005) Deregulation of cell proliferation by polycyclic aromatic hydrocarbons in human breast carcinoma MCF-7 cells reflects both genotoxic and nongenotoxic events. *Toxicol. Sci.*, 83, 246–256.
77. Hockley, S.L. *et al.* (2006) Time- and concentration-dependent changes in gene expression induced by benzo(a)pyrene in two human cell lines, MCF-7 and HepG2. *BMC Genomics*, 7, 260.
78. Matthews, J. *et al.* (2006) Estrogen receptor and aryl hydrocarbon receptor signaling pathways. *Nucl. Recept. Signal.*, 4, e016.
79. Ahmed, S. *et al.* (2009) Dioxin increases the interaction between aryl hydrocarbon receptor and estrogen receptor alpha at human promoters. *Toxicol. Sci.*, 111, 254–266.
80. Madak-Erdogan, Z. *et al.* (2012) Aryl hydrocarbon receptor modulation of estrogen receptor α-mediated gene regulation by a multimeric chromatin complex involving the two receptors and the coregulator RIP140. *Toxicol. Sci.*, 125, 401–411.
81. Richmond, O. *et al.* (2014) The aryl hydrocarbon receptor is constitutively active in advanced prostate cancer cells. *PLoS One*, 9, e95058.
82. Schlezinger, J.J. *et al.* (2006) A role for the aryl hydrocarbon receptor in mammary gland tumorigenesis. *Biol. Chem.*, 387, 1175–1187.
83. Yang, X. *et al.* (2008) Constitutive regulation of CYP1B1 by the aryl hydrocarbon receptor (AhR) in pre-malignant and malignant mammary tissue. *J. Cell. Biochem.*, 104, 402–417.